PERGAMON

International Journal of Solids and Structures 38 (2001) 8219–8233

INTERNATIONAL JOURNAL OF SOLIDS and STRUCTURES

www.elsevier.com/locate/ijsolstr

An edge dislocation interacting with a wedge-shaped bi-material interface

Z.M. Xiao *, B.J. Chen, H. Fan

School of Mechanical & Production Engineering, Nanyang Technological University, Nanyang Avenue, Singapore 639798, Singapore

Received 29 November 2000; in revised form 18 May 2001

Abstract

The elastic stress field due to an edge dislocation near the tip of a wedge-shaped bi-material interface is derived using the conformal mapping method. The stress intensity factors of the wedge tip induced by the dislocation, the interaction strain energy, and the imaging force acting on the dislocation are formulated and calculated. The influences of the wedge angle and the different bi-material combinations on the imaging force are discussed.

Keywords: Edge dislocation; Interaction; Wedge-shaped interface; Stress intensity factor; Force on dislocation

1. Introduction

In engineering materials and structures, wedge-shaped interfaces are very often encountered, such as in polycrystalline materials, composite materials with irregular inclusions, and square silicon die encapsulated by epoxy matrix in electronic packages, etc. As a wedge-shaped interface introduces stress singularity at its corner where a micro-crack could be easily initiated, a number of researchers have been studying on such problems for the last two decades. To give some examples, Bogy and Wang (1971) investigated the problem of a composite body consisting of two dissimilar isotropic, homogeneous wedges. In their work, an eigen equation for determining the order of singularity at the corner of wedge shaped interface was given. The same problem was restudied by Chen and Nisitani (1993), in which an explicit closed form expression was established for the singular stress field at the corner. Reedy and Guess (1997) analyzed the critical value of the stress singularity intensity at a wedge corner for a micro crack to be initiated. Reedy (2000) further studied the connection between the failure criteria based on the critical values of singularity intensity factor at the wedge corner and the traditional stress intensity factor. Recently Pahn and Earmme (2000) investigated the problem for a crack initiated from the corner of a rectangular inclusion.

* Corresponding author. Fax: +65-791-1859.
E-mail address: mzxiao@ntu.edu.sg (Z.M. Xiao).

0020-7683/01/$ - see front matter
PII: S0020-7683(01)00143-3

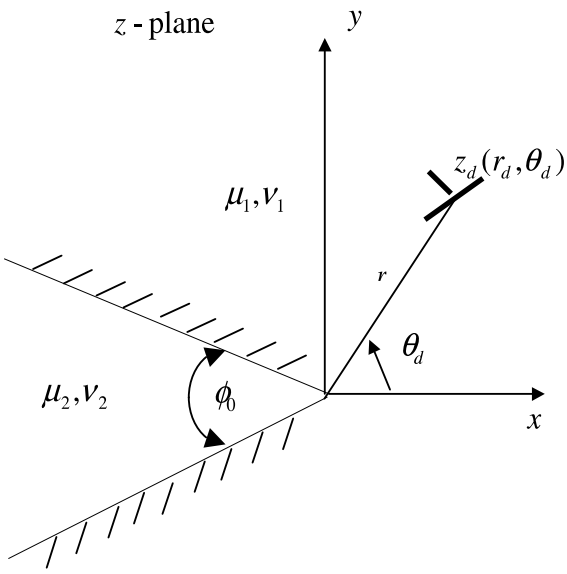

Fig. 1. An edge dislocation near a wedge shape inhomogeneity.

The objective of the present paper is to obtain the stress solution for a single edge dislocation near a wedge-shaped bi-material interface as shown in Fig. 1. Since a crack in solid can be simulated by a distribution of dislocations along the crack face (Weertman, 1996), the current solution can be used as the Green's function to study interaction problems for a crack near a wedge corner. A lot of research work on dislocation–inclusion (interface) interaction can be found in open literature, it is worth to have a brief review here. The early contributions up to 1960s to this area were summarized by Dundurs (1969a), where he summarized the single dislocation in an infinite solid, a dislocation in a bi-material space (dislocation in a half spaces is the special case by taking one of the material as zero modulus), a dislocation interacting with a circular inclusion. More recently, Lo (1978) studied the interaction between a dislocation with a crack when he conducted research on crack branching. Warren (1983) considered the interaction between a single dislocation with an elliptical inclusion via conformal mapping technique. Dundurs and Markenscoff (1989) gave the solution for a dislocation interacting with an anti-crack (rigid line inclusion). Xiao and Chen (2001) tackled the interaction between a dislocation and an inclusion coated with different type of materials. It is not difficult to see that all the above mentioned configurations have significant physical applications in modeling of defects in solid materials.

In the following sections, we shall present the solution for a single dislocation in bi-material space as shown in Fig. 1. It is apparent that the geometric configuration in Fig. 1 can be reduced to joint-two-half space, anti-crack, and a crack by taking special value of ϕ_0 and special modulus for one of the materials, therefore the aforementioned existing results can be used as checking for our derivations. During the solution procedure the conformal mapping technique was employed, with which the wedge configuration as shown in Fig. 1 is mapped onto two-joint-half spaces. Due to the complexity of the formulation, a symbolic derivation program, MATHEMATICA (Wolfram, 1996), was used to minimize possible mistakes. Based upon the Green's function obtained, we found the force acting on the dislocation which drives the dislocation toward or away from the wedge corner. Also, since the stress at the corner of the wedge is singular, we calculated the stress intensity factor due to the presence of the dislocation.

2. Formulation and complex potentials of the problem

The physical problem to be investigated is shown in Fig. 1. Both materials are assumed to be isotropic and linear elastic, and extend infinitely in the x-axis direction. The wedge angle is denoted as ϕ_0. An edge dislocation with Burgers vector $b = b_x + \mathrm{i}b_y$ is located at $z_\mathrm{d}(r_\mathrm{d}, \theta_\mathrm{d})$ in the Material 1. The shear modulus and Poisson's ratio of the bi-material combinations are denoted by μ_1, v_1 and μ_2, v_2 respectively.

The continuum conditions along the interface $\theta = \pm(\pi - \phi_0/2)$ are

$$(u_\theta^1 - \mathrm{i}u_r^1) - (u_\theta^2 - \mathrm{i}u_r^2) = 0, \tag{2.1a}$$

$$(\sigma_{r\theta}^1 - \mathrm{i}\sigma_{\theta\theta}^1) - (\sigma_{r\theta}^2 - \mathrm{i}\sigma_{\theta\theta}^2) = 0, \tag{2.1b}$$

where the superscripts "1" and "2" denote the variables for the Material 1 and 2, respectively. We assume plane strain state, so that the displacement and stress components can be written in terms of two complex potentials $\varphi(z)$ and $\psi(z)$ (Muskhelishvili, 1975).

$$2\mu(u + \mathrm{i}v) = \kappa\varphi(z) - z\overline{\varphi'(z)} - \overline{\psi(z)}, \tag{2.2a}$$

$$\sigma_{xx} - \mathrm{i}\sigma_{xy} = \varphi'(z) + \overline{\varphi'(z)} - \bar{z}\varphi''(z) - \psi'(z), \tag{2.2b}$$

$$\sigma_{yy} + \mathrm{i}\sigma_{xy} = \varphi'(z) + \overline{\varphi'(z)} + \bar{z}\varphi''(z) + \psi'(z), \tag{2.2c}$$

where $\kappa = 3 - 4v$. The over bar denotes a complex conjugate, and the prime denotes differentiation with respect to the argument z. Our task now becomes to find the complex functions $\varphi_1(z)$, $\varphi_2(z)$, $\psi_1(z)$ and $\psi_2(z)$, from which the displacement and stress components in the two regions must satisfy the continuity conditions (2.1a,b).

By choosing a conformal mapping function as

$$z = w(\varsigma) = \varsigma^{1/q}, \tag{2.3}$$

with $q = \pi/(2\pi - \phi_0)$ and $\varsigma = \xi + \mathrm{i}\eta$, this function maps the interface $\theta = \pm(\pi - \phi_0/2)$ in the z-plane of Fig. 1 into the imaginary axis in the ς-plane, as shown in Fig. 2. Let the four complex potentials have the following forms in the ς-plane

$$\varphi_1 = \gamma[\ln(\varsigma - \varsigma_\mathrm{d}) + \Pi\ln(-\varsigma - \bar{\varsigma}_\mathrm{d})] + \varphi_{10}, \tag{2.4a}$$

$$\psi_1 = \bar{\gamma}[\ln(\varsigma - \varsigma_\mathrm{d}) + \Lambda\ln(-\varsigma - \bar{\varsigma}_\mathrm{d})] + \psi_{10}, \tag{2.4b}$$

$$\varphi_2 = \gamma(1 + \Lambda)\ln(\varsigma - \varsigma_\mathrm{d}) + \varphi_{20}, \tag{2.4c}$$

$$\psi_2 = \bar{\gamma}(1 + \Pi)\ln(\varsigma - \varsigma_\mathrm{d}) + \psi_{20}, \tag{2.4d}$$

where

$$\gamma = \frac{\mu_1}{\pi(1 + \kappa_1)}(b_y - \mathrm{i}b_x), \tag{2.5a}$$

$$\Lambda = (\alpha + \beta)/(1 - \beta), \tag{2.5b}$$

$$\Pi = (\alpha - \beta)/(1 + \beta), \tag{2.5c}$$

with α and β as the Dundurs' bi-material parameters (Dundurs, 1969a). Following Muskhelishvili (1975), the continuum conditions (2.1a) and (2.1b) can be rewritten in terms of the complex potentials as

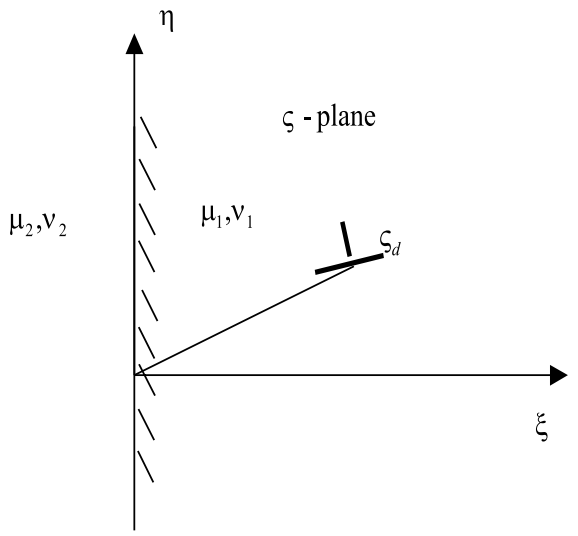

Fig. 2. An edge dislocation near a straight line interface.

$$\Gamma\left[\kappa_1\overline{\varphi_1(\varsigma_c)}-\overline{\frac{w(\varsigma_c)}{w'(\varsigma_c)}}\varphi_1'(\varsigma_c)-\psi_1(\varsigma_c)\right]-\left[\kappa_2\overline{\varphi_2(\varsigma_c)}-\overline{\frac{w(\varsigma_c)}{w'(\varsigma_c)}}\varphi_2'(\varsigma_c)-\psi_2(\varsigma_c)\right]=0, \tag{2.6a}$$

$$\left[\overline{\varphi_1(\varsigma_c)}+\overline{\frac{w(\varsigma_c)}{w'(\varsigma_c)}}\varphi_1'(\varsigma_c)+\psi_1(\varsigma_c)\right]-\left[\overline{\varphi_2(\varsigma_c)}+\overline{\frac{w(\varsigma_c)}{w'(\varsigma_c)}}\varphi_2'(\varsigma_c)+\psi_2(\varsigma_c)\right]=0, \tag{2.6b}$$

where ς_c lies on the interface (i.e. $\varsigma_c=i\eta$), and

$$\Gamma=\frac{\mu_2}{\mu_1}. \tag{2.7}$$

Substituting Eqs. (2.4a)–(2.4d), into Eqs. (2.6a) and (2.6b) and using the relationship

$$\kappa_1=\frac{\Gamma(1+\beta)-(1+\alpha)}{(\alpha-\beta)\Gamma},\qquad \kappa_2=\frac{\Gamma(1-\alpha)-(1-\beta)}{\alpha-\beta}, \tag{2.8}$$

we obtain

$$\psi_{10}(\varsigma_c)=\frac{1}{\Pi}\overline{\varphi_{10}(\varsigma_c)}-\frac{1-\Lambda\Pi}{\Pi(1+\Lambda)}\overline{\varphi_{20}(\varsigma_c)}-\overline{\frac{w(\varsigma_c)}{w'(\varsigma_c)}}\varphi_1'(\varsigma_c), \tag{2.9a}$$

$$\psi_{20}(\varsigma_c)=\frac{1+\Pi}{\Pi}\overline{\varphi_{10}(\varsigma_c)}-1+\frac{1+\Pi}{\Pi(1+\Lambda)}\overline{\varphi_{20}(\varsigma_c)}-\overline{\frac{w(\varsigma_c)}{w'(\varsigma_c)}}\varphi_2'(\varsigma_c). \tag{2.9b}$$

Since $\bar{\varsigma}_c=-\varsigma_c$ holds on the imaginary axis of the ς-plane, we have

$$\psi_{10}(\varsigma)=\frac{1}{\Pi}\bar{\varphi}_{10}(-\varsigma)-\frac{1-\Lambda\Pi}{\Pi(1+\Lambda)}\bar{\varphi}_{20}(-\varsigma)-\frac{\bar{w}(-\varsigma)}{w'(\varsigma)}\varphi_1'(\varsigma), \tag{2.10a}$$

$$\psi_{20}(\varsigma)=\frac{1+\Pi}{\Pi}\bar{\varphi}_{10}(-\varsigma)+\frac{1+\Pi}{\Pi(1+\Lambda)}\bar{\varphi}_{20}(-\varsigma)-\frac{\bar{w}(-\varsigma)}{w'(\varsigma)}\varphi_2'(\varsigma). \tag{2.10b}$$

Substituting Eqs. (2.4a), (2.4b) and (2.9a) into Eq. (2.2a), we obtain the displacement in the Material 1 as

$$\begin{aligned}2\mu_1(u_1+\mathrm{i}v_1)=\kappa_1\gamma[\ln(\varsigma-\varsigma_\mathrm{d})+\Pi\ln(\varsigma-\bar{\varsigma}_\mathrm{d})]-\gamma[\ln(\bar{\varsigma}-\bar{\varsigma}_\mathrm{d})+\Lambda\ln(-\bar{\varsigma}-\varsigma_\mathrm{d})]\\ -\frac{w(\varsigma)-w(-\bar{\varsigma})}{\overline{w'(\varsigma)}}\bar{\gamma}\left[\frac{1}{\bar{\varsigma}-\bar{\varsigma}_\mathrm{d}}+\frac{\Pi}{-\bar{\varsigma}-\varsigma_\mathrm{d}}\right]-\frac{1}{\Pi}\varphi_{10}(-\bar{\varsigma})+\frac{1-\Lambda\Pi}{\Pi(1+\Lambda)}\varphi_{20}(-\bar{\varsigma})\\ -\frac{w(\varsigma)-w(-\bar{\varsigma})}{\overline{w'(\varsigma)}}\overline{\varphi'_{10}(\varsigma)}+\kappa_1\varphi_{10}(\varsigma),\end{aligned}\tag{2.11}$$

According to the physical nature of a dislocation, only the singularity in the logarithmic term is allowed when $\varsigma\to\varsigma_\mathrm{d}$. Thus, in order to cancel the singularity in the other term, φ_{10} and φ_{20} are chosen as

$$\varphi_{10}(\varsigma)=\frac{w(\varsigma_\mathrm{d})-w(-\bar{\varsigma}_\mathrm{d})}{\overline{w'(\varsigma_\mathrm{d})}}\frac{\Pi\bar{\gamma}}{\varsigma+\bar{\varsigma}_\mathrm{d}},\tag{2.12a}$$

$$\varphi_{20}=0.\tag{2.12b}$$

Since

$$\begin{aligned}&w(\varsigma)=(\varsigma)^{1/q}=z,\qquad w(-\varsigma)=(-\varsigma)^{1/q}=\mathrm{e}^{\mathrm{i}\pi/q}z=\mathrm{e}^{-\mathrm{i}\phi_0}z,\\ &w(-\bar{\varsigma})=\mathrm{e}^{-\phi_0}\bar{z},\qquad w'(\varsigma)=\frac{1}{q}(\varsigma)^{1/q-1}=\frac{1}{q}z^{1-q}.\end{aligned}\tag{2.13}$$

Eq. (2.12a) is rewritten as

$$\varphi_{10}(z)=\frac{(z_\mathrm{d}-\mathrm{e}^{-\mathrm{i}\phi_0}\bar{z}_\mathrm{d})\bar{z}_\mathrm{d}^{q-1}q\Pi\bar{\gamma}}{z^q+\bar{z}_\mathrm{d}^q}.\tag{2.14}$$

Substitution of the above equations into Eqs. (2.10a) and (2.10b) arrives at

$$\psi_{10}=\frac{(\mathrm{e}^{\mathrm{i}\phi_0}z_\mathrm{d}-\bar{z}_\mathrm{d})z_\mathrm{d}^{q-1}q\gamma}{z^q-z_\mathrm{d}^q}-\frac{\mathrm{e}^{\mathrm{i}\phi_0}z^q q\gamma}{z^q-z_\mathrm{d}^q}-\frac{\mathrm{e}^{\mathrm{i}\phi_0}z^q q\Pi\gamma}{z^q+\bar{z}_\mathrm{d}^q}+\frac{(\mathrm{e}^{\mathrm{i}\phi_0}z_\mathrm{d}-\bar{z}_\mathrm{d})z_\mathrm{d}^{q-1}z^q q^2\Pi\bar{\gamma}}{(z^q+z_\mathrm{d}^q)^2},\tag{2.15a}$$

$$\psi_{20}=\frac{(\mathrm{e}^{\mathrm{i}\phi_0}z_\mathrm{d}-\bar{z}_\mathrm{d})z_\mathrm{d}^{q-1}q(1+\Pi)\gamma}{z^q-z_\mathrm{d}^q}-\frac{\mathrm{e}^{\mathrm{i}\phi_0}z^q q(1+\Lambda)\gamma}{z^q-z_\mathrm{d}^q}.\tag{2.15b}$$

Finally, the complex potentials for the current problem are obtained as

$$\varphi_1(z)=\gamma\ln(z^q-z_\mathrm{d}^q)+\Pi\gamma\ln(-z^q-\bar{z}_\mathrm{d}^q)+\frac{(z_\mathrm{d}-\mathrm{e}^{-\mathrm{i}\phi_0}\bar{z}_\mathrm{d})\bar{z}_\mathrm{d}^{q-1}q\Pi\bar{\gamma}}{z^q+\bar{z}_\mathrm{d}^q},\tag{2.16a}$$

$$\varphi_2(z)=\gamma(1+\Lambda)\ln(z^q-z_\mathrm{d}^q),\tag{2.16b}$$

$$\begin{aligned}\psi_1(z)=\bar{\gamma}\ln(z^q-z_\mathrm{d}^q)+\Lambda\bar{\gamma}\ln(-z^q-\bar{z}_\mathrm{d}^q)+\frac{(\mathrm{e}^{\mathrm{i}\phi_0}z_\mathrm{d}-\bar{z}_\mathrm{d})z_\mathrm{d}^{q-1}q\gamma}{z^q-z_\mathrm{d}^q}-\frac{\mathrm{e}^{\mathrm{i}\phi_0}z^q q\gamma}{z^q-z_\mathrm{d}^q}-\frac{\mathrm{e}^{\mathrm{i}\phi_0}z^q q\Pi\gamma}{z^q+\bar{z}_\mathrm{d}^q}\\ +\frac{(\mathrm{e}^{\mathrm{i}\phi_0}z_\mathrm{d}-\bar{z}_\mathrm{d})z_\mathrm{d}^{q-1}z^q q^2\Pi\bar{\gamma}}{(z^q+\bar{z}_\mathrm{d}^q)^2},\end{aligned}\tag{2.16c}$$

$$\psi_2(z)=\bar{\gamma}(1+\Pi)\ln(z^q-z_\mathrm{d}^q)+\frac{(\mathrm{e}^{\mathrm{i}\phi_0}z_\mathrm{d}-\bar{z}_\mathrm{d})z_\mathrm{d}^{q-1}q(1+\Pi)\gamma}{z^q-z_\mathrm{d}^q}-\frac{\mathrm{e}^{\mathrm{i}\phi_0}z^q q(1+\Lambda)\gamma}{z^q-z_\mathrm{d}^q}.\tag{2.16d}$$

It is noticed that the results given in Eqs. (2.16a)–(2.16d) can be reduced to those of an edge dislocation near a straight interface (Dundurs, 1969b) by setting $q = 1$ ($\phi_0 = \pi$). The present results can also be reduced to those of an edge dislocation near a wedge crack (Zhang and Tong, 1995) by setting Material 2 as zero modulus.

3. Displacement and stress fields

With the aids of Eqs. (2.2a)–(2.2c) and (2.4a)–(2.4d) the displacements and stress fields in Fig. 1 due to the edge dislocation can be calculated. For example, the stress field in the matrix phase can be calculated by using Eqs. (2.16a) and (2.16c), given by

$$\sigma_{xx} = \frac{\mu_1}{\pi(1+\kappa_1)}(h_{xxx}b_x + h_{xxy}b_y), \tag{3.1a}$$

$$\sigma_{yy} = \frac{\mu_1}{\pi(1+\kappa_1)}(h_{yyx}b_x + h_{yyy}b_y), \tag{3.1b}$$

$$\sigma_{xy} = \frac{\mu_1}{\pi(1+\kappa_1)}(h_{xyx}b_x + h_{xyy}b_y), \tag{3.1c}$$

where the expressions of h_{xxx}, h_{xxy}, h_{yyx}, h_{yyy}, h_{xyx}, h_{xyy} are listed in the Appendix A.

It is worth to point out that the tedious expressions in Eqs. (3.1a)–(3.1c) can be checked by some special cases (Dundurs and Markenscoff, 1989) for the Green's function formulation of anticracks. This is made by letting $\phi_0 = 0$, $\theta = \theta_d = 0$, and $\Gamma = \mu_2/\mu_1 \to \infty$. In this case, $\alpha = 1$, $\beta = (\kappa_1 - 1)/(\kappa_1 + 1)$, from Eqs. (3.1a)–(3.1c), we obtain the stress components on the real axis due to an edge dislocation located at the real axis. For example, the normal stress component on the real axis due to a climb edge dislocation located at the real axis in this case is

$$\sigma_{yy}(x,0) = \frac{\mu_1 b_y}{2\pi\kappa_1(\kappa_1+1)(x-r_d)}\left[(\kappa_1+1)^2 - (\kappa_1-1)^2\sqrt{\frac{r_d}{x}}\right], \tag{3.2}$$

which is the same as the result given by Dundurs and Markenscoff (1989) for the case of a semi-infinite anticrack.

From Eqs. (3.1a)–(3.1c), the stresses are found to be singular at the corner of the wedge. If we define the stress intensity factors as

$$K_I + \mathrm{i}K_{II} = \lim_{z\to 0}(z)^{1-q}(\sigma_{yy} + \mathrm{i}\sigma_{xy}), \tag{3.3}$$

z approaches the origin along the positive real axis. Substituting Eq. (2.2c) into Eq. (3.3) with Eqs. (2.16a) and (2.16c), we have

$$\begin{aligned} K_I + \mathrm{i}K_{II} = &\left[\frac{\bar{z}_d(1-\Pi) + z_d(\mathrm{e}^{\mathrm{i}\phi_0}\Pi - 1)}{z_d^{1+q}} - \frac{(\mathrm{e}^{\mathrm{i}\phi_0}-1)\Pi}{\bar{z}_d^{q}}\right]q^2\gamma \\ &+ \left[\frac{q^2 z_d \Pi(\mathrm{e}^{\mathrm{i}\phi_0}-1)}{\bar{z}_d^{1+q}} + \frac{\Lambda - 1 + (\mathrm{e}^{-\mathrm{i}\phi_0}-1)q^2\Pi}{\bar{z}_d^{q}} + \frac{\Pi - 1}{z_d^{q}}\right]q\bar{\gamma}. \end{aligned} \tag{3.4}$$

If the dislocation is located at the x-axis, Eq. (3.4) is simplified as

$$K_I + \mathrm{i}K_{II} = \frac{q\bar{\gamma}}{z_d^{q}}[\Pi + \Lambda - 2 - 2q^2\Pi(1-\cos\phi_0)]. \tag{3.5}$$

In the case of a wedge crack (i.e. $\Pi = \Lambda = -1$), Eq. (3.5) is further reduced to

$$K_I + \mathrm{i}K_{II} = \frac{q\bar{\gamma}}{z_{\mathrm{d}}^{q}}[2q^2(1-\cos\phi_0)]. \tag{3.6}$$

The above equation coincides with the result derived by Zhang and Tong (1995) for an edge dislocation near a wedge crack.

4. The strain energy and force on the dislocation

The strain energy of the edge dislocation per unit length is evaluated as the work required to move the dislocation in the material. With reference to Fig. 1, we have

$$W = \mathrm{Re}\left\{\frac{1}{2}(b_x + \mathrm{i}b_y)\int_{r_{\mathrm{d}}\cos\theta_{\mathrm{d}}+r_0}^{R}[\sigma_{xy}(x, r_{\mathrm{d}}\sin\theta_{\mathrm{d}}) + \mathrm{i}\sigma_{yy}(x, r_{\mathrm{d}}\sin\theta_{\mathrm{d}})]\,\mathrm{d}x\right\}, \tag{4.1}$$

where R is the distance corresponding to the material size and r_0 is the core radius of the dislocation. We may take $R \to \infty$ and $r_0 \to 0$ for all the convergent terms in the integrals.

The integrals in Eq. (4.1) can be written in terms of the complex potentials (Muskhelishvili, 1975) as

$$\int_{r_{\mathrm{d}}\cos\theta_{\mathrm{d}}+r_0}^{R}[\sigma_{xy}(x, r_{\mathrm{d}}\sin\theta_{\mathrm{d}}) + \mathrm{i}\sigma_{yy}(x, r_{\mathrm{d}}\sin\theta_{\mathrm{d}})]\,\mathrm{d}x = -\mathrm{i}[\varphi_1(z) + z\overline{\varphi_1'(z)} + \overline{\psi_1(z)}]\Big|_{z_{\mathrm{d}}}^{z_\infty}, \tag{4.2}$$

where z_∞ is obtained by letting $z_\infty = x + r_{\mathrm{d}}\cos\theta_{\mathrm{d}}$, with $x \to +\infty$. Substituting Eq. (2.14) into the above equation, and discarding the divergent terms associated with the self-energy, we finally arrive at

$$W = \frac{\mu_1}{2\pi(\kappa_1+1)}[(b_x^2 + b_y^2)c_1 + (b_x^2 - b_y^2)c_2 + 2b_x b_y c_3], \tag{4.3}$$

where

$$c_1 = [2 - q(2 + \Lambda + \Pi)]\ln r_{\mathrm{d}} - (\Lambda + \Pi)\ln(2\cos q\theta_{\mathrm{d}}) + q^2\Pi\sec^2 q\theta_{\mathrm{d}}\sin^2\left(\frac{\phi_0}{2} + \theta_{\mathrm{d}}\right), \tag{4.4a}$$

$$c_2 = q\{(1+\Pi)(\cos\phi_0 - 1) + \Pi\sec q\theta_{\mathrm{d}}[\cos(q-2)\theta_{\mathrm{d}} - \cos(q\theta_{\mathrm{d}} + \phi_0)]\}, \tag{4.4b}$$

$$c_3 = -q\{(1+\Pi)\sin\phi_0 + \Pi\sec q\theta_{\mathrm{d}}[\sin(q-2)\theta_{\mathrm{d}} - \sin(q\theta_{\mathrm{d}} + \phi_0)]\}, \tag{4.4c}$$

The image force on the edge dislocation is defined as a negative gradient of the strain energy with respect to the position of the dislocation. The radial and tangential components of the image force per unit length are then given by

$$F_r = -\frac{\partial W}{\partial r_{\mathrm{d}}}, \qquad F_\theta = -\frac{1}{r_{\mathrm{d}}}\frac{\partial W}{\partial \theta_{\mathrm{d}}}. \tag{4.5}$$

Substituting Eq. (4.3) into Eqs. (4.4a)–(4.4c) yields

$$F_r = -\frac{\mu_1(b_x^2 + b_y^2)}{2\pi(\kappa_1+1)}\frac{2 - q(2+\Lambda+\Pi)}{r_{\mathrm{d}}}, \tag{4.6}$$

$$F_\theta = -\frac{\mu_1}{2\pi(\kappa_1+1)}\frac{(b_x^2 + b_y^2)d_1 + (b_x^2 - b_y^2)d_2 + 2b_x b_y d_3}{r_{\mathrm{d}}}, \tag{4.7}$$

where

$$d_1 = q\{(\Lambda + \Pi)\tan q\theta_d + q\Pi \sec^2 q\theta_d \sin(\alpha_0 + 2\theta_d) + q^2\Pi \sec^2 q\theta_d[1 - \cos(\phi_0 + 2\theta_d)]\tan q\theta_d\}, \tag{4.8a}$$

$$d_2 = q\Pi \sec^2 q\theta_d[q \sin\phi_0 + (q-1)\sin 2\theta_d + \sin 2(q-1)\theta_d], \tag{4.8b}$$

$$d_3 = q\Pi \sec^2 q\theta_d[q \cos\phi_0 - q\cos 2\theta_d + 2\cos q\theta_d \cos(2-q)\theta_d]. \tag{4.8c}$$

5. Numerical examples and discussions

So far we have obtained the exact expression for the stress intensity factors (SIFs) induced by the edge dislocation in Eq. (3.4) and the exact expression for the forces on the edge dislocation in Eq. (4.6) to Eqs. (4.8a)–(4.8c). They are functions of wedge angle $\phi_0(q)$, bi-material constants Π, Λ, Burgers vectors $b_x + ib_y$ and the location of the edge dislocation (r_d, θ_d). In order to have a better understanding on how these parameters influence on the SIFs and the force on the dislocation, the following numerical examples are given and plotted in this section. Four typical material combinations are used:

(I) $\Pi = \Lambda = -1$, wedge crack;
(II) $\Pi = -0.65$, $\Lambda = -0.35$, Material 1 is "harder" than Material 2;
(III) $\Pi = 2.55$, $\Lambda = 0.27$, Material 1 is "softer" than Material 2;
(IV) $\Pi = 3.33$, $\Lambda = 0.30$, wedge anti-crack.

5.1. Stress intensity factor

Here we consider an edge dislocation with Burgers vector $b_x + ib_y = be^{i\theta_b}$, where θ_b is chosen to equal to θ_d for calculation. The Mode I SIF arising from such an edge dislocation as a function of distance r_d from the tip of the dislocation when the Material 1 is "harder" than Material 2 is plotted in Fig. 3. It is found that when the dislocation is along the real axis, no Mode I SIF is induced. The magnitudes of Mode I SIFs increase from zero to a maximum as θ_d increases from 0° to $\theta_{d\,max}$ and then decrease to zero as θ_d continues to increase. The same phenomena can be observed when the Material 1 is "softer" than Material 2. But this

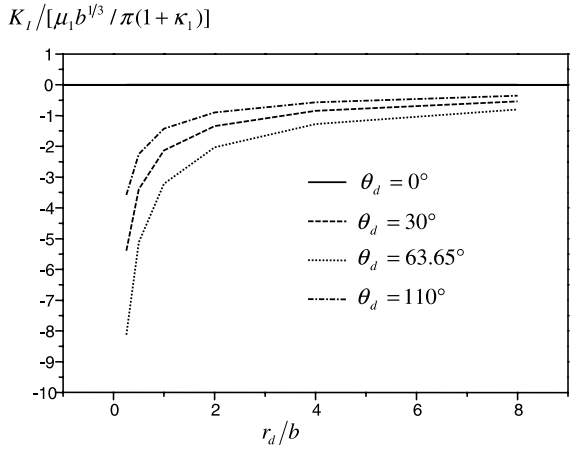

Fig. 3. Normalized Mode I SIF arising from an edge dislocation of Burgers vector $b_x + ib_y = be^{i\theta_d}$ at $\Pi = -0.65$, $\Lambda = -0.35$, $\phi_0 = 90°$.

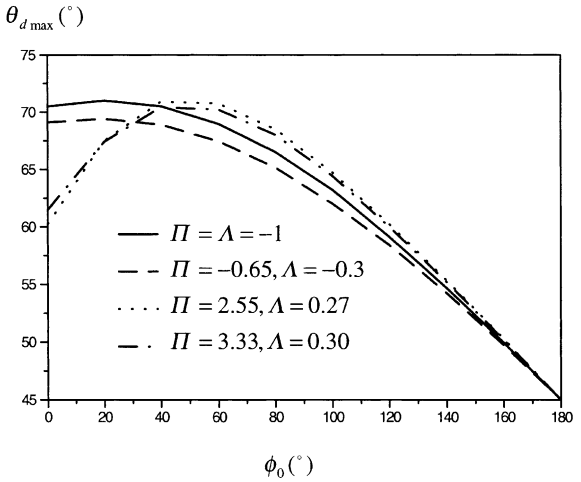

Fig. 4. The slip plane of an edge dislocation with Burgers vector $b_x + \mathrm{i}b_y = b\mathrm{e}^{\mathrm{i}\theta_{\mathrm{d\,max}}}$ corresponding to the maximum Mode I SIF.

is not true for Mode II SIF. Fig. 4 shows the slip plane of an edge dislocation inclined at $\theta_{\mathrm{d\,max}}$ corresponding to the maximum magnitude of Mode I SIF as a function wedge angle ϕ_0. $\theta_{\mathrm{d\,max}}$ increases from a value to a maximum and then decreases to 45° as ϕ_0 increases from 0° to 180°. This is obvious when Material 1 is "softer" than Material 2.

5.2. Force on the dislocation

Eq. (4.6) indicates that the radial component of the image force is independent of θ_{d}. Thus, the wedge tip always repels the edge dislocation in the radial direction when

$$2/q < 2 + \Pi + \Lambda, \tag{5.1}$$

and attracts the edge dislocation in the radial direction when

$$2/q > 2 + \Pi + \Lambda. \tag{5.2}$$

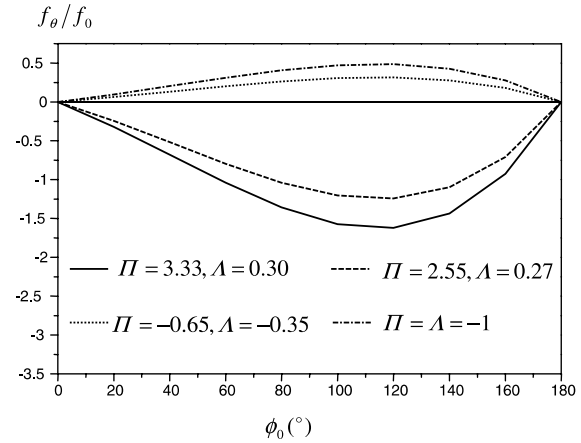

Fig. 5. Normalized tangential force on the gliding edge dislocation of Burgers vector b_x located at $\theta_{\mathrm{d}} = 0°$.

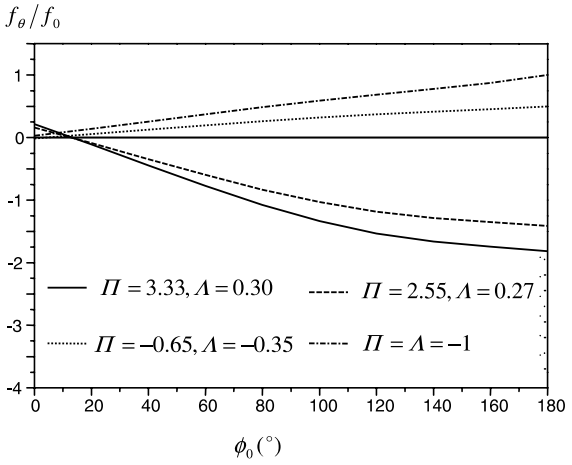

Fig. 6. Normalized tangential force on the gliding edge dislocation of Burgers vector b_x located at $\theta_d = 45°$.

However, the tangential component of the image force is dependent of θ_d. Fig. 5 shows the tangential component of the image force f_θ as a function of the wedge angle ϕ_0 at $\theta_d = 0°$ for the gliding edge dislocation. Fig. 6 shows the tangential component of the image force f_θ as a function of the wedge angle ϕ_0 at $\theta_d = 45°$ for the gliding edge dislocation. The image force in the figures are normalized by

$$f_0 = \frac{\mu_1 b_x^2}{\pi(1+\kappa_1)}, \tag{5.3}$$

It is found that when the dislocation is at the real axis, f_θ is always negative when the Material 2 is "harder" than the Material 1, and is always positive when the Material 2 is "softer". Its amplitude increases from zero to a maximum and then decreases to zero as the wedge angle increases from 0° to 180°. But this is not true when the dislocation is not located at the real axis.

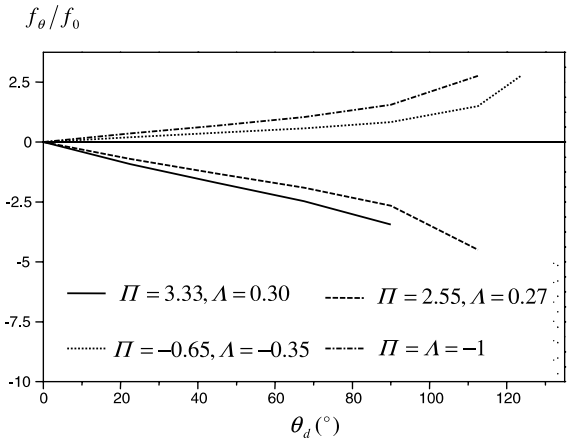

Fig. 7. Normalized tangential force on the climbing edge dislocation of Burgers vector b_y located at $\phi_0 = 90°$.

In order to study the influence on f_θ from the dislocation location, the normalized f_θ is plotted as a function of θ_d in Fig. 7 for a climbing edge dislocation, when $\phi_0 = 90°$. For the climbing edge dislocation, the amplitude of f_θ increases gradually from zero as θ_d increases from 0° to 90° and then increases quickly as θ_d increases from 90°.

6. Concluding remarks

The problem of an edge dislocation interacting with a wedge-shaped bi-material interface is solved using the conformal mapping method. With accordance to the physical nature of a dislocation and the continuity condition along the interface, the Muskhelishvili complex potentials for the problem are determined. The stress intensity factor of the wedge tip, and the force on the dislocation are calculated and discussed. The present solutions are successfully reduced to some simple cases existing in the open literature (Dundurs and Markenscoff, 1989; Zhang and Tong, 1995).

Appendix A

$$h_{xxx} = qr^{q-1}(2\,\mathrm{im}s1 + 2\,\mathrm{im}s2 - 2\,\mathrm{im}s3 - \mathrm{im}s4 - \mathrm{im}s5 - \mathrm{im}s6 - \mathrm{im}s7 + \mathrm{im}s8 + \mathrm{im}s9 + \mathrm{im}s10 + \mathrm{im}s11 - \mathrm{im}s12 + \mathrm{im}s13 - \mathrm{im}s14 + \mathrm{im}s15), \tag{A.1}$$

$$h_{xxy} = qr^{q-1}(2\,\mathrm{re}s1 + 2\,\mathrm{re}s2 + 2\,\mathrm{re}s3 - \mathrm{re}s4 - \mathrm{re}s5 - \mathrm{re}s6 - \mathrm{re}s7 - \mathrm{re}s8 - \mathrm{re}s9 - \mathrm{re}s10 - \mathrm{re}s11 - \mathrm{re}s12 - \mathrm{re}s13 - \mathrm{re}s14 - \mathrm{re}s15), \tag{A.2}$$

$$h_{yyx} = qr^{q-1}(2\,\mathrm{im}s1 + 2\,\mathrm{im}s2 - 2\,\mathrm{im}s3 + \mathrm{im}s4 + \mathrm{im}s5 + \mathrm{im}s6 + \mathrm{im}s7 - \mathrm{im}s8 - \mathrm{im}s9 - \mathrm{im}s10 - \mathrm{im}s11 + \mathrm{im}s12 - \mathrm{im}s13 + \mathrm{im}s14 - \mathrm{im}s15), \tag{A.3}$$

$$h_{yyy} = qr^{q-1}(2\,\mathrm{re}s1 + 2\,\mathrm{re}s2 + 2\,\mathrm{re}s3 + \mathrm{re}s4 + \mathrm{re}s5 + \mathrm{re}s6 + \mathrm{re}s7 + \mathrm{re}s8 + \mathrm{re}s9 + \mathrm{re}s10 + \mathrm{re}s11 + \mathrm{re}s12 + \mathrm{re}s13 + \mathrm{re}s14 + \mathrm{re}s15), \tag{A.4}$$

$$h_{xyx} = qr^{q-1}(-\mathrm{re}s4 - \mathrm{re}s5 - \mathrm{re}s6 - \mathrm{re}s7 + \mathrm{re}s8 + \mathrm{re}s9 + \mathrm{re}s10 + \mathrm{re}s11 - \mathrm{re}s12 + \mathrm{re}s13 - \mathrm{re}s14 + \mathrm{re}s15), \tag{A.5}$$

$$h_{xyy} = qr^{q-1}(\mathrm{im}s4 + \mathrm{im}s5 + \mathrm{im}s6 + \mathrm{im}s7 + \mathrm{im}s8 + \mathrm{im}s9 + \mathrm{im}s10 + \mathrm{im}s11 + \mathrm{im}s12 + \mathrm{im}s13 + \mathrm{im}s14 + \mathrm{im}s15), \tag{A.6}$$

where

$$\mathrm{re}s1 = \frac{r^q\cos\theta - r_d^q\cos(\theta - q\theta + q\theta_d)}{r^{2q} + r_d^{2q} - 2r^q r_d^q\cos q(\theta - \theta_d)}, \tag{A.7}$$

$$\mathrm{im}s1 = \frac{-r^q\sin\theta + r_d^q\sin(\theta - q\theta + q\theta_d)}{r^{2q} + r_d^{2q} - 2r^q r_d^q\cos q(\theta - \theta_d\theta_d)}, \tag{A.8}$$

$$\mathrm{re}s2 = \frac{\Pi[r^q\cos\theta + r_d^q\cos(\theta - q\theta - q\theta_d)]}{r^{2q} + r_d^{2q} + 2r^q r_d^q\cos q(\theta + \theta_d)}, \tag{A.9}$$

$$\mathrm{im}\,s2 = -\frac{\Pi[r^q \sin\theta + r_\mathrm{d}^q \sin(\theta - q\theta - q\theta_\mathrm{d})]}{r^{2q} + r_\mathrm{d}^{2q} + 2r^q r_\mathrm{d}^q \cos q(\theta + \theta_\mathrm{d})}, \tag{A.10}$$

$$\mathrm{re}\,s3 = -\frac{2q\Pi r_\mathrm{d}^q \sin\left(\frac{\phi_0}{2} + \theta_\mathrm{d}\right)}{\left[r^{2q} + r_\mathrm{d}^{2q} + 2r^q r_\mathrm{d}^q \cos q(\theta + \theta_\mathrm{d})\right]^2}\left\{2r^q r_\mathrm{d}^q \sin\left(\frac{\phi_0}{2} + \theta - \theta_\mathrm{d}\right)\right.$$
$$\left. + r_\mathrm{d}^{2q} \sin\left[\frac{\phi_0}{2} + (1-q)\theta - (1+q)\theta_\mathrm{d}\right] + r^{2q} \sin\left[\frac{\phi_0}{2} + (1+q)\theta - (1-q)\theta_\mathrm{d}\right]\right\}, \tag{A.11}$$

$$\mathrm{im}\,s3 = -\frac{2q\Pi r_\mathrm{d}^q \sin\left(\frac{\phi_0}{2} + \theta_\mathrm{d}\right)}{\left[r^{2q} + r_\mathrm{d}^{2q} + 2r^q r_\mathrm{d}^q \cos q(\theta + \theta_\mathrm{d})\right]^2}\left\{2r^q r_\mathrm{d}^q \cos\left(\frac{\phi_0}{2} + \theta - \theta_\mathrm{d}\right)\right.$$
$$\left. + r_\mathrm{d}^{2q} \cos\left[\frac{\phi_0}{2} + (1-q)\theta - (1+q)\theta_\mathrm{d}\right] + r^{2q} \cos\left[\frac{\phi_0}{2} + (1+q)\theta - (1-q)\theta_\mathrm{d}\right]\right\}, \tag{A.12}$$

$$\mathrm{re}\,s4 = \frac{-r^q \cos 3\theta + r_\mathrm{d}^q \cos(q\theta - 3\theta - q\theta_\mathrm{d})}{r^{2q} + r_\mathrm{d}^{2q} - 2r^q r_\mathrm{d}^q \cos q(\theta - \theta_\mathrm{d})}, \tag{A.13}$$

$$\mathrm{im}\,s4 = \frac{r^q \sin 3\theta + r_\mathrm{d}^q \sin(q\theta - 3\theta - q\theta_\mathrm{d})}{r^{2q} + r_\mathrm{d}^{2q} - 2r^q r_\mathrm{d}^q \cos q(\theta - \theta_\mathrm{d})}, \tag{A.14}$$

$$\mathrm{re}\,s5 = -\frac{\Pi[r^q \cos 3\theta + r_\mathrm{d}^q \cos(q\theta - 3\theta + q\theta_\mathrm{d})]}{r^{2q} + r_\mathrm{d}^{2q} + 2r^q r_\mathrm{d}^q \cos q(\theta + \theta_\mathrm{d})}, \tag{A.15}$$

$$\mathrm{im}\,s5 = \frac{\Pi[r^q \cos 3\theta - r_\mathrm{d}^q \cos(q\theta - 3\theta + q\theta_\mathrm{d})]}{r^{2q} + r_\mathrm{d}^{2q} + 2r^q r_\mathrm{d}^q \cos q(\theta + \theta_\mathrm{d})}, \tag{A.16}$$

$$\mathrm{re}\,s6 = -\frac{qr_\mathrm{d}^q[-2r^q r_\mathrm{d}^q \cos 3\theta + r^{2q} \cos(q\theta + 3\theta - q\theta_\mathrm{d}) + r_\mathrm{d}^{2q} \cos(q\theta - 3\theta - q\theta_\mathrm{d})]}{\left[r^{2q} + r_\mathrm{d}^{2q} - 2r^q r_\mathrm{d}^q \cos q(\theta - \theta_\mathrm{d})\right]^2}, \tag{A.17}$$

$$\mathrm{im}\,s6 = \frac{qr_\mathrm{d}^q[-2r^q r_\mathrm{d}^q \sin 3\theta + r^{2q} \sin(q\theta + 3\theta - q\theta_\mathrm{d}) - r_\mathrm{d}^{2q} \sin(q\theta - 3\theta - q\theta_\mathrm{d})]}{\left[r^{2q} + r_\mathrm{d}^{2q} - 2r^q r_\mathrm{d}^q \cos q(\theta - \theta_\mathrm{d})\right]^2}, \tag{A.18}$$

$$\mathrm{re}\,s7 = \frac{qr_\mathrm{d}^q \Pi[2r^q r_\mathrm{d}^q \cos 3\theta + r^{2q} \cos(q\theta + 3\theta + q\theta_\mathrm{d}) + r_\mathrm{d}^{2q} \cos(q\theta - 3\theta + q\theta_\mathrm{d})]}{\left[r^{2q} + r_\mathrm{d}^{2q} + 2r^q r_\mathrm{d}^q \cos q(\theta + \theta_\mathrm{d})\right]^2}, \tag{A.19}$$

$$\mathrm{im}\,s7 = -\frac{qr_\mathrm{d}^q \Pi[2r^q r_\mathrm{d}^q \sin 3\theta + r^{2q} \sin(q\theta + 3\theta + q\theta_\mathrm{d}) - r_\mathrm{d}^{2q} \sin(q\theta - 3\theta + q\theta_\mathrm{d})]}{\left[r^{2q} + r_\mathrm{d}^{2q} + 2r^q r_\mathrm{d}^q \cos q(\theta + \theta_\mathrm{d})\right]^2}, \tag{A.20}$$

$$\mathrm{re}\,s8 = \frac{2q(1+q)\Pi r_\mathrm{d}^q \sin\left(\frac{\phi_0}{2} + \theta_\mathrm{d}\right)}{\left[r^{2q} + r_\mathrm{d}^{2q} + 2r^q r_\mathrm{d}^q \cos q(\theta + \theta_\mathrm{d})\right]^2}\left\{2r^q r_\mathrm{d}^q \sin\left(\frac{\phi_0}{2} + 3\theta - \theta_\mathrm{d}\right)\right.$$
$$\left. + r_\mathrm{d}^{2q} \sin\left[\frac{\phi_0}{2} - (q-3)\theta - (q+1)\theta_\mathrm{d}\right] + r^{2q} \sin\left[\frac{\phi_0}{2} + (3+q)\theta + (q-1)\theta_\mathrm{d}\right]\right\}, \tag{A.21}$$

$$\mathrm{im}\,s8 = \frac{2q(1+q)\Pi r_{\mathrm{d}}^{q}\sin\left(\frac{\phi_0}{2}+\theta_{\mathrm{d}}\right)}{[r^{2q}+r_{\mathrm{d}}^{2q}+2r^{q}r_{\mathrm{d}}^{q}\cos q(\theta+\theta_{\mathrm{d}})]^{2}}\left\{2r^{q}r_{\mathrm{d}}^{q}\cos\left(\frac{\phi_0}{2}+3\theta-\theta_{\mathrm{d}}\right)\right.$$
$$\left.+\,r_{\mathrm{d}}^{2q}\cos\left[\frac{\phi_0}{2}-(q-3)\theta-(q+1)\theta_{\mathrm{d}}\right]+r^{2q}\cos\left[\frac{\phi_0}{2}+(3+q)\theta+(q-1)\theta_{\mathrm{d}}\right]\right\}, \tag{A.22}$$

$$\mathrm{re}\,s9 = -\frac{4q^{2}\Pi r_{\mathrm{d}}^{2q}\sin\left(\frac{\phi_0}{2}+\theta_{\mathrm{d}}\right)}{[r^{2q}+r_{\mathrm{d}}^{2q}+2r^{q}r_{\mathrm{d}}^{q}\cos q(\theta+\phi)]^{3}}\left\{3r^{q}r_{\mathrm{d}}^{2q}\sin\left(\frac{\phi_0}{2}+3\theta-\theta_{\mathrm{d}}\right)\right.$$
$$+\,3r^{2q}r_{\mathrm{d}}^{q}\sin\left[\frac{\phi_0}{2}+(q+3)\theta+(q-1)\theta_{\mathrm{d}}\right]+r_{\mathrm{d}}^{3q}\sin\left(\frac{\phi_0}{2}+3\theta-q\theta-\theta_{\mathrm{d}}-q\theta_{\mathrm{d}}\right)$$
$$\left.+\,r^{3q}\sin\left(\frac{\phi_0}{2}+3\theta+2q\theta-\theta_{\mathrm{d}}+2q\theta_{\mathrm{d}}\right)\right\}, \tag{A.23}$$

$$\mathrm{im}\,s9 = -\frac{4q^{2}\Pi r_{\mathrm{d}}^{2q}\sin\left(\frac{\phi_0}{2}+\theta_{\mathrm{d}}\right)}{[r^{2q}+\rho^{2q}+2r^{q}\rho^{q}\cos q(\theta+\theta_{\mathrm{d}})]^{3}}\left\{3r^{q}r_{\mathrm{d}}^{2q}\cos\left(\frac{\phi_0}{2}+3\theta-\theta_{\mathrm{d}}\right)\right.$$
$$+\,3r^{2q}r_{\mathrm{d}}^{q}\cos\left[\frac{\phi_0}{2}+(q+3)\theta+(q-1)\theta_{\mathrm{d}}\right]$$
$$\left.+\,r_{\mathrm{d}}^{3q}\cos\left(\frac{\phi_0}{2}+3\theta-q\theta-\theta_{\mathrm{d}}-q\theta_{\mathrm{d}}\right)+r^{3q}\cos\left(\frac{\phi_0}{2}+3\theta+2q\theta-\theta_{\mathrm{d}}+2q\theta_{\mathrm{d}}\right)\right\}, \tag{A.24}$$

$$\mathrm{re}\,s10 = \frac{r^{q}\cos\theta-r_{\mathrm{d}}^{q}\cos(\theta-q\theta+q\theta_{\mathrm{d}})}{r^{2q}+r_{\mathrm{d}}^{2q}-2r^{q}r_{\mathrm{d}}^{q}\cos q(\theta-\theta_{\mathrm{d}})}, \tag{A.25}$$

$$\mathrm{im}\,s10 = \frac{-r^{q}\sin\theta+r_{\mathrm{d}}^{q}\sin(\theta-q\theta+q\theta_{\mathrm{d}})}{r^{2q}+r_{\mathrm{d}}^{2q}-2r^{q}r_{\mathrm{d}}^{q}\cos q(\theta-\theta_{\mathrm{d}})}, \tag{A.26}$$

$$\mathrm{re}\,s11 = \frac{\Lambda[r^{q}\cos\theta+r_{\mathrm{d}}^{q}\cos(\theta-q\theta-q\theta_{\mathrm{d}})]}{r^{2q}+r_{\mathrm{d}}^{2q}+2r^{q}r_{\mathrm{d}}^{q}\cos q(\theta+\theta_{\mathrm{d}})}, \tag{A.27}$$

$$\mathrm{im}\,s11 = -\frac{\Lambda[r^{q}\sin\theta+r_{\mathrm{d}}^{q}\sin(\theta-q\theta-q\theta_{\mathrm{d}})]}{r^{2q}+r_{\mathrm{d}}^{2q}+2r^{q}r_{\mathrm{d}}^{q}\cos q(\theta+\theta_{\mathrm{d}})}, \tag{A.28}$$

$$\mathrm{re}\,s12 = -\frac{qr_{\mathrm{d}}^{q}}{[r^{2q}+r_{\mathrm{d}}^{2q}-2r^{q}r_{\mathrm{d}}^{q}\cos q(\theta-\theta_{\mathrm{d}})]^{2}}[-2r^{q}r_{\mathrm{d}}^{q}\cos(\theta+2\theta_{\mathrm{d}})+r^{2q}\cos(q\theta+\theta+2\theta_{\mathrm{d}}-q\theta_{\mathrm{d}})$$
$$+\,r_{\mathrm{d}}^{2q}\cos(q\theta-\theta-2\theta_{\mathrm{d}}-q\theta_{\mathrm{d}})], \tag{A.29}$$

$$\mathrm{im}\,s12 = \frac{qr_{\mathrm{d}}^{q}}{[r^{2q}+r_{\mathrm{d}}^{2q}-2r^{q}r_{\mathrm{d}}^{q}\cos q(\theta-\theta_{\mathrm{d}})]^{2}}[2r^{q}r_{\mathrm{d}}^{q}\sin(\theta+2\theta_{\mathrm{d}})-r^{2q}\sin(q\theta+\theta+2\theta_{\mathrm{d}}-q\theta_{\mathrm{d}})$$
$$+\,r_{\mathrm{d}}^{2q}\sin(q\theta-\theta-2\theta_{\mathrm{d}}-q\theta_{\mathrm{d}})], \tag{A.30}$$

$$\mathrm{re}\,s13 = \frac{2q^{2}\Pi r_{\mathrm{d}}^{q}\sin\left(\frac{\phi_0}{2}+\theta_{\mathrm{d}}\right)}{[r^{2q}+r_{\mathrm{d}}^{2q}+2r^{q}r_{\mathrm{d}}^{q}\cos q(\theta+\phi)]^{2}}\left\{2r^{q}r_{\mathrm{d}}^{q}\sin\left(\frac{\phi_0}{2}-\theta+\theta_{\mathrm{d}}\right)\right.$$
$$\left.+\,r_{\mathrm{d}}^{2q}\sin\left[\frac{\phi_0}{2}+(q-1)\theta+(q+1)\theta_{\mathrm{d}}\right]+r^{2q}\sin\left[\frac{\phi_0}{2}-(q+1)\theta-(q-1)\theta_{\mathrm{d}}\right]\right\}, \tag{A.31}$$

$$\mathrm{im}\,s13 = -\frac{2q^2\Pi r_{\mathrm{d}}^{q}\sin\left(\frac{\phi_0}{2}+\theta_{\mathrm{d}}\right)}{\left[r^{2q}+r_{\mathrm{d}}^{2q}+2r^{q}r_{\mathrm{d}}^{q}\cos q(\theta+\theta_{\mathrm{d}})\right]^2}\left\{2r^{q}r_{\mathrm{d}}^{q}\cos\left(\frac{\phi_0}{2}-\theta+\theta_{\mathrm{d}}\right)\right.$$
$$\left.+\,r_{\mathrm{d}}^{2q}\cos\left[\frac{\phi_0}{2}+(q-1)\theta+(q+1)\theta_{\mathrm{d}}\right]+r^{2q}\cos\left[\frac{\phi_0}{2}-(q+1)\theta-(q-1)\theta_{\mathrm{d}}\right]\right\}, \tag{A.32}$$

$$\mathrm{re}\,s14 = -\frac{qr_{\mathrm{d}}^{q}\Pi}{\left[r^{2q}+r_{\mathrm{d}}^{2q}+2r^{q}r_{\mathrm{d}}^{q}\cos q(\theta+\theta_{\mathrm{d}})\right]^2}[2r^{q}r_{\mathrm{d}}^{q}\cos(\phi_0-\theta)+r^{2q}\cos(\phi_0-q\theta-\theta-q\theta_{\mathrm{d}})$$
$$+\,r_{\mathrm{d}}^{2q}\cos(\phi_0+q\theta-\theta+q\theta_{\mathrm{d}})], \tag{A.33}$$

$$\mathrm{im}\,s14 = -\frac{qr_{\mathrm{d}}^{q}\Pi}{\left[r^{2q}+r_{\mathrm{d}}^{2q}+2r^{q}r_{\mathrm{d}}^{q}\cos q(\theta+\theta_{\mathrm{d}})\right]^2}[2r^{q}r_{\mathrm{d}}^{q}\sin(\phi_0-\theta)+r^{2q}\sin(\phi_0-q\theta-\theta-q\theta_{\mathrm{d}})$$
$$+\,r_{\mathrm{d}}^{2q}\sin(\phi_0+q\theta-\theta+q\theta_{\mathrm{d}})], \tag{A.34}$$

$$\mathrm{re}\,s15 = -\frac{4q^2\Pi r_{\mathrm{d}}^{2q}\sin\left(\frac{\phi_0}{2}+\theta_{\mathrm{d}}\right)}{\left[r^{2q}+r_{\mathrm{d}}^{2q}+2r^{q}r_{\mathrm{d}}^{q}\cos q(\theta+\theta_{\mathrm{d}})\right]^3}\left\{3r^{q}r_{\mathrm{d}}^{2q}\sin\left(\frac{\phi_0}{2}-\theta+\theta_{\mathrm{d}}\right)\right.$$
$$+\,3r^{2q}r_{\mathrm{d}}^{q}\sin\left[\frac{\phi_0}{2}-(q+1)\theta-(q-1)\theta_{\mathrm{d}}\right]+r_{\mathrm{d}}^{3q}\sin\left(\frac{\phi_0}{2}-\theta+q\theta+\theta_{\mathrm{d}}+q\theta_{\mathrm{d}}\right)$$
$$\left.+\,r^{3q}\sin\left(\frac{\phi_0}{2}-\theta-2q\theta+\theta_{\mathrm{d}}-2q\theta_{\mathrm{d}}\right)\right\}, \tag{A.35}$$

$$\mathrm{im}\,s15 = \frac{4q^2\Pi r_{\mathrm{d}}^{2q}\sin\left(\frac{\phi_0}{2}+\theta_{\mathrm{d}}\right)}{\left[r^{2q}+r_{\mathrm{d}}^{2q}+2r^{q}r_{\mathrm{d}}^{q}\cos q(\theta+\theta_{\mathrm{d}})\right]^3}\left\{3r^{q}r_{\mathrm{d}}^{2q}\cos\left(\frac{\phi_0}{2}-\theta+\theta_{\mathrm{d}}\right)\right.$$
$$+\,3r^{2q}r_{\mathrm{d}}^{q}\cos\left[\frac{\phi_0}{2}-(q+1)\theta-(q-1)\theta_{\mathrm{d}}\right]+r_{\mathrm{d}}^{3q}\cos\left(\frac{\phi_0}{2}-\theta+q\theta+\theta_{\mathrm{d}}+q\theta_{\mathrm{d}}\right)$$
$$\left.+\,r^{3q}\cos\left(\frac{\phi_0}{2}-\theta-2q\theta+\theta_{\mathrm{d}}-2q\theta_{\mathrm{d}}\right)\right\}. \tag{A.36}$$

References

Bogy, D.B., Wang, K.C., 1971. Stress singularities at interface corners in bonded dissimilar isotropic elastic materials. International Journal of Solids and Structures 7, 993–1005.

Chen, D.H., Nisitani, H., 1993. Singular stress field near the corner of jointed dissimilar materials. Journal of Applied Mechanics 60, 607–613.

Dundurs, J., 1969a. Discussion of a paper by D.B. Bogy. Journal of Applied Mechanics 36, 650–652.

Dundurs, J., 1969b. Elastic interaction of dislocations with inhomogeneities, Mathematical Theory of Dislocation. ASME, New York, pp. 70–115.

Dundurs, J., Markenscoff, X., 1989. A Green's function formulation of anticracks and their interaction with load-induced singularities. Journal of Applied Mechanics 56, 550–555.

Lo, K.K., 1978. Analysis of branched cracks. Journal of Applied Mechanics 45 (4), 797–802.

Muskhelishvili, N.I., 1975. Some Basic Problems of the Mathematical Theory of Elasticity. Noordhoff International Publishing, Leyden.

Pahn, L.O., Earmme, Y.Y., 2000. Analysis of a short interfacial crack from the corner of a rectangular inclusion. International Journal of Fracture 106, 341–356.

Reedy, E.D., 2000. Connection between interface corner and interfacial fracture analyses of an adhesively-bonded butt joint. International Journal of Solids and Structure 37, 2429–2442.

Reedy, E.D., Guess, T.R., 1997. Interface corner failure analysis of joint strength: effect of adherend stiffness. International Journal of Fracture 88, 305–314.
Warren, William E., 1983. Edge dislocation inside an elliptical inclusion. Mechanics of Materials 2 (4), 319–330.
Weertman, J., 1996. Dislocation Based Fracture Mechanics. World Scientific publishing.
Wolfram, S., 1996. The Mathematica Book, third ed. Wolfram Media/Cambridge University Press, Cambridge, MA.
Xiao, Z.M., Chen, B.J., 2001. On the interaction between an edge dislocation and a coated inclusion. International Journal of Solids and Structures 38 (15), 2533–2548.
Zhang, T.Y., Tong, P., 1995. Interaction of an edge dislocation with a wedge crack. Journal of Applied Physics 78, 4783–4880.